



## Effect of nanostructuring frictional treatment on the properties of high-carbon pearlitic steel. Part II: mechanical properties



R.A. Savrai<sup>a,\*</sup>, A.V. Makarov<sup>a,b,c</sup>

<sup>a</sup> Institute of Engineering Science, Ural Branch, Russian Academy of Sciences, 34 Komsomolskaya St., Yekaterinburg 620049, Russia

<sup>b</sup> M.N. Miheev Institute of Metal Physics, Ural Branch, Russian Academy of Sciences, 18 S.Kovalevskaya St., Yekaterinburg 620108, Russia

<sup>c</sup> Ural Federal University, 19 Mira St., Yekaterinburg 620002, Russia

### ARTICLE INFO

#### Keywords:

High-carbon pearlitic steel  
Frictional treatment  
Static tension  
Contact fatigue

### ABSTRACT

In this second part of the work, the mechanical properties, features of deformation and fracture under static and contact fatigue loading of the high-carbon (1.03 wt% C) steel with a fine-lamellar pearlitic structure have been studied before and after frictional treatment with a sliding indenter. It has been found that the frictional treatment practically does not affect the mechanical properties of the steel under static tension. A method of contact fatigue testing for estimating the contact endurance of thin hardened surface layers has been proposed, which consists in performing contact fatigue tests according to a pulsing non-impact “sphere-to-surface” contact scheme under conditions of repeated elastic-plastic deformation with different maximum loads. It has been established that the frictional treatment increases the fracture resistance of the steel surface under contact fatigue loading, if contact damages are localized in the thin surface layer with maximum hardness and high values of microindentation based parameters. However, the hardened surface layer can endure heavy contact loads until failure and fractures only when contact damages cover the entire layer.

### 1. Introduction

Fine-lamellar pearlite in carbon steels has a unique ability to sustain significant plastic strain, which is widely used in practice to perform bulk deformation, for example, in the production of high-strength wire [1]. As applied to pearlitic carbon steels, some studies of the effect of deformation on their structure and properties are known from the literature, in particular, the effect of deformation by high pressure torsion on fracture toughness [2], high pressure torsion and sliding friction on the structure and microhardness of high-carbon steels with pearlitic structures [3,4]. The effect of severe plastic deformation by equal-channel angular pressing (ECAP) on the structure [5] and mechanical characteristics [6,7] of these steels is considered as well. The behavior of high-carbon pearlitic steels under static and cyclic tension is also investigated [8,9]. Nevertheless, the features of deformation and fracture of severe surface deformed high-carbon pearlitic steels under various mechanical actions have yet to be studied more thoroughly.

Also, pearlitic carbon steels are widely used in railway transport, where contact fatigue is one of the most dangerous forms of fatigue fracture [1]. The processes of fatigue fracture in solids under repeated mechanical contact are more complex than processes occurring under ordinary fatigue loading. Besides crack formation and evolution,

friction and wear processes take place under contact fatigue loading, as well as a complex stress state in the contact zone [10]. In this connection, contact endurance tests become of great importance. Cyclic strength of materials under conditions of mechanical contact is estimated through various tests, among which rolling contact fatigue testing is the most widespread. To estimate the contact endurance of coatings and materials, pulsing contact fatigue testing can also be effective [11–15], since crack nucleation starts from the surface under this type of loading, as distinct from rolling, where much contribution to failure is made by subsurface defects [16–18].

The aim of this second part of the work is to study the mechanical properties, features of deformation and fracture under static and contact fatigue loading of the high-carbon (1.03 wt% C) steel with a fine-lamellar pearlitic structure before and after frictional treatment with a sliding indenter. In the first part of this work, it has been shown that, as compared to heat treatment, the nanostructuring frictional treatment of the high-carbon (1.03 wt% C) steel with a fine-lamellar pearlitic structure must increase resistance of the steel to intensive mechanical contact [19]. In this second part, the experimental verification of the ability of the high-carbon steel with different structural states of its surface to withstand contact loads was performed.

\* Corresponding author.

E-mail address: [ras@imach.uran.ru](mailto:ras@imach.uran.ru) (R.A. Savrai).

<https://doi.org/10.1016/j.msea.2018.07.100>

Received 31 May 2018; Received in revised form 23 July 2018; Accepted 27 July 2018

Available online 29 July 2018

0921-5093/© 2018 Elsevier B.V. All rights reserved.

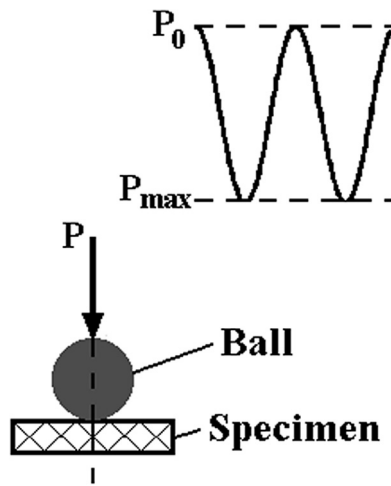


Fig. 1. Scheme of mechanical tests for contact fatigue.

## 2. Experimental procedure

In this second part of the work, commercial high-carbon steel GOST U10 presented in the first part was studied. The steel was processed following the same procedure as that described in the first part of this work [19].

Mechanical tests for static tension and contact fatigue were made on an Instron 8801 servohydraulic machine. Contact fatigue tests were performed with the use of a fixture of unique design [20] according to the pulsing non-impact “sphere-to-surface” contact scheme, with a steel ball diameter of 12.7 mm, preload  $P_0 = 0.1$  kN, maximum load  $P_{max} = 1.09, 1.7, 2.54, 3.62, 4.99, 6.67$  and  $8.7$  kN, loading frequency  $f = 35$  Hz on the basis of  $N = 10^6$  loading cycles, the loading in a cycle being varied according to the periodic (sine) law (Fig. 1).

Contact stresses were calculated according to the Hertzian contact theory [21] for the elastic contact between the sphere and the plane having identical elastic moduli  $E_1 = E_2 = E = 210$  GPa and the Poisson's ratios  $\nu_1 = \nu_2 = \nu = 0.3$ :

$$\sigma_{z \max} = 0.3883 \sqrt{P \frac{E^2}{R^2}}, \quad (1)$$

where  $\sigma_{z \max}$  is maximum normal stress in the contact zone, MPa;  $P$  is normal load, N;  $E$  is the elastic modulus of the contacting bodies, MPa;  $R$  is sphere radius, mm.

The depth of the experimental contact spots was calculated by the formula:

$$h = R - \frac{R^2}{d} \sin \alpha, \quad \alpha = 2 \arcsin \left( \frac{d}{2R} \right), \quad (2)$$

where  $h$  is contact spot depth, mm;  $d$  is contact spot diameter, mm.

Contact spots after contact fatigue tests were examined with the use of Tescan LYRA 3 GMU scanning electron microscope (SEM) with energy-dispersive microanalysis system (EDS).

## 3. Results and discussion

Table 1 shows that frictional treatment practically does not affect the mechanical properties of the high-carbon steel with a fine-lamellar pearlitic structure, unlike the annealed low-carbon (0.17 wt% C) [22,23] or quenched and tempered medium-carbon (0.51 wt% C) [24,25] steels. At that, 0.2% proof strength  $S_{p0.2}$  and ultimate tensile strength  $S_u$  change only slightly, fracture stress  $S_{tot}$  increases by 65 MPa, uniform elongation  $\delta_u$  remains practically unchanged, total elongation  $\delta_{tot}$  decreases by 1.4%, remaining fairly high ( $\delta_{tot} = 7.2\%$ ). The shape of the stress-strain diagram also remains unchanged, and the specimen flow remains uniform during plastic deformation (Fig. 2). Note that the

Table 1

Strength (0.2% proof strength  $S_{p0.2}$ , ultimate tensile strength  $S_u$ , fracture stress  $S_{tot}$ ) and plasticity (uniform elongation  $\delta_u$ , total elongation  $\delta_{tot}$ ) characteristics under static tension of the high-carbon steel with a fine-lamellar pearlitic structure.

Processing	$S_{p0.2}$ , MPa	$S_u$ , MPa	$S_{tot}$ , MPa	$\delta_u$ , %	$\delta_{tot}$ , %
Before frictional treatment	$1080 \pm 10$	$1510 \pm 5$	$1425 \pm 10$	$6.5 \pm 0.2$	$8.6 \pm 0.4$
After frictional treatment	$1080 \pm 10$	$1515 \pm 5$	$1480 \pm 10$	$6.2 \pm 0.3$	$7.2 \pm 0.7$

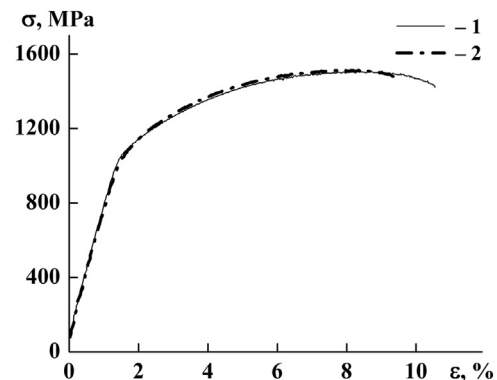


Fig. 2. Stress-strain diagrams under uniaxial tension for the high-carbon steel with a fine-lamellar pearlitic structure before (1) and after (2) frictional treatment.

uniform flow at the initial stage of deformation under static tension is characteristic of the steels after frictional and combined strain-heat treatments. This consists in disappearance of the upper yield point and yield plateau in the annealed low-carbon steel [22,23], and yield plateau in the quenched and tempered medium-carbon steel [24,25]. Nonuniform material flow at the initial stage of deformation under static tension is characteristic of a coarsely dispersed structure, and it stems from the absence of distributed stress mesoconcentrators in the bulk of the specimen and, consequently, a limited material volume simultaneously involved in the plastic flow [26,27]. In this case, as a rule, tensile deformation at the initial loading stage develops through the frontal propagation of one mesoband of localized strain (Lüders-Chernov band). The structure of fine-lamellar pearlite is highly dispersed (see Figs. 2, 4c and d in part I [19]), and after frictional treatment, an even more dispersed nanocrystalline structure is formed in the steel (see Figs. 4a, 5 in part I [19]). Accordingly, such structures have long grain or interphase boundaries. The boundaries are stress concentrators, and their relaxation causes the involvement of a larger material volume into plastic flow [28,29], this being manifested in the uniform flow of the steel at the initial stage of deformation under static tension (see Fig. 2). Some decrease in the value of total elongation after frictional treatment may be due to surface microcracking, which contributes to a more rapid specimen fracture once localized necking is started [24].

Thus, as compared to heat treatment alone, this frictional treatment has no significant effect on tensile properties of the steel. This is most likely due to a relatively small depth of the effective hardening ( $50 \mu\text{m}$ ) [19], which on both sides of the specimen does not exceed 5% from the specimen thickness (2.2 mm).

The results of the calculation of contact stresses and contact spot depths are presented in Table 2. Note that the value of contact stresses  $\sigma_{z \max}$  can several times exceed ultimate tensile strength  $S_u$  (see Table 1). According to the theory of elasticity, the ability of materials to withstand high contact stresses stems from the fact that the most

Download English Version:

<https://daneshyari.com/en/article/11007045>

Download Persian Version:

<https://daneshyari.com/article/11007045>

[Daneshyari.com](https://daneshyari.com)